Large Events in Waves on the Continental Shelf

Large Events in Waves on the Continental Shelf

Mohd. R.M. Haniffah[1], Paul H. Taylor[2], Chris Swan[3], Vanessa Katsardi[3,4], Alistair G.L. Borthwick[5]
[1]Faculty of Civil Engineering, Universiti Teknologi Malaysia, Malaysia
[2]Department of Engineering Science, University of Oxford, Parks Road, Oxford OX1 3PJ, U.K.
[3]Department of Civil and Environmental Engineering, Imperial College, London, SW7 2AZ, U.K.
[4]Department of Civil Engineering, University of Thessaly, Greece
[5]School of Engineering, The University of Edinburgh, Edinburgh, EH9 3JL, Scotland
…
email: mridza@utm.my, paul.taylor@eng.ox.ac.uk, c.swan@imperial.ac.uk, vkatsardi@civ.uth.gr, alistair.borthwick@ed.ac.uk

ABSTRACT: Offshore structures located on the continental shelf experience loading from locally extreme events in storm-induced wave groups as they shoal. This paper examines modern developments in assessing the transformations that take place to ocean wave spectra as the bathymetry shallows, and examines laboratory data obtained from tests undertaken at Imperial College London on random waves as they travel over gently sloping beds. The data show that NewWave provides a satisfactory fit to the largest crest- and trough- focused events in all depths of water, until wave breaking occurs. The paper also considers how well NewWave models the linear behavior of extreme waves in shallowing water, and presents results from a Stokes-like expansion accounting for the asymmetry of large waves. It is shown that the largest crest elevations, lowest trough elevations, and breaking wave heights are all limited by a modified Miche criterion. The findings should be useful to offshore engineers required to assess the air gap elevation of structures located on the continental shelf.

KEY WORDS: Offshore structures; Extreme waves; NewWave; Limiting height.

1 INTRODUCTION

The continental shelf comprises a gently sloping landmass that extends outwards from the coastal shoreline to a depth of about 140 m beyond which the ocean depth rapidly increases. Many offshore oil and gas platforms, maritime jetties, and other structures are located on the continental shelf, and are subject to loading from storm-driven waves that shoal as they travel inshore from the deep ocean waters. Engineers are required to design structures whose decks are above the level of the highest wave crest elevation and whose support structures can withstand the most extreme wave loadings. This paper addresses the former problem by considering the use of a focused wave methodology to represent non-breaking extreme wave events, and limiting elevation/height criteria to design for breaking and broken waves.

For more than 20 years, NewWave has been used in the design of deep water offshore structures. The NewWave concept originated from statistical theory aimed at determining the shape of the extreme event in a time history related to a given spectrum [1], [2], was applied to ocean waves by Tromans and colleagues [3]. The idea of a wave group proved useful for numerical simulation, [4], and for the analysis of wave data from the open sea, [5], [6]. It was validated through meticulous laboratory experiments by Rapp and Melville [7], Baldock *et al*. [8], Johannessen and Swan [9], [10], amongst others. The free surface elevation of a focused wave group is given by NewWave as

$$\eta_{\mathrm{NW}}(t) = A\frac{\int S(\omega)\cos\omega t\,\mathrm{d}\omega}{\int S(\omega)\,\mathrm{d}\omega} \qquad (1)$$

in which A is the wave amplitude of the focused wave group, $S(\omega)$ is the wave energy spectral density at wave angular frequency ω, and t is time.

As storm-driven waves pass over the continental shelf, they shoal, their crests narrow and troughs broaden, and as the water depth reduces they break. Miche [11] obtained a limiting height criterion for waves passing over a horizontal bed, which Katsardi [12] modified for very mild slopes, giving

$$H_{\max} = 0.12\,\lambda\tanh kd \qquad (2)$$

in which $H_{\max}$ is the wave height at breaking, λ is the wave length, k is the wave number, and d is the local water depth.

In the mid-2000s, a series of laboratory tests were undertaken at Imperial College, London, as part of a Joint Industry Project to assess extreme wave behaviour over mild slopes in shallow water. This paper presents some of the measurements, and describes how the data were interpreted in terms of large events. A Stokes-like expansion approach is used to study the harmonic structure of the wave free surface elevation time history. The paper briefly outlines the laboratory test facility and the wave gauge instrumentation before separately considering non-breaking and broken wave behaviour. The possible use of NewWave and the modified Miche criterion to represent such events is considered.

2 IMPERIAL COLLEGE WAVE FLUME

Irregular waves were generated in a 60 m long flume of width 0.3 m, where the still water depth was 0.7 m at the paddles. Tests were undertaken for three beach configurations, one a raised horizontal bed with constant still water depth of 0.3 m along its length, the second a 1:100 plane beach with toe still water depth of 0.5 m, and the third a 1:250 plane beach with toe still water depth of 0.3 m. A transitional bed ramp of slope 1:15 joined the bed at the paddles to the beaches. A series of resistance-type wave gauges were located along the flume centreline, providing measurements of the water surface level, accurate to within 0.5 mm.

Irregular wave trains were generated, corresponding to a JONSWAP spectrum with a peak enhancement factor of $\gamma = 2.5$; with all other properties being listed in Table 1). In each case, measurements were collected at 128 Hz for an ensemble of eight free surface elevation time histories, each lasting 256 s. The resulting time series included 1200 to 1700 waves covering a total duration of 2048 s. Further details are given by Katsardi [12] and Katsardi et al. [13]

Table 1. Input parameters.

Case	Bed Slope	T_p (s)	H_{so} (m)
Case A1a	1/100	1.2	96.0
Case A1b	1/100	1.2	120.2
Case A3a	1/100	1.5	11.2
Case A3b	1/100	1.5	29.2
Case A3c	1/100	1.5	83.3
Case A3d	1/100	1.5	102.9
Case A3e	1/100	1.5	121.3
Case B1b	1/250	1.2	119.1
Case B3e	1/250	1.5	122.2
Case C1b	Horizontal	1.2	120.1
Case C3e	Horizontal	1.5	128.9

3 RESULTS

3.1 Largest Free Surface Events in Time

We first consider the free surface elevation behaviour at three gauges, G2 where d = 0.35 m, G6 where d = 0.15 m, and G8 where d = 0.05 m. Figure 1 shows portions of the time histories of free surface elevation obtained at each of these gauges. In the deeper water at G2, the waves are more sinusoidal in form. In the shallower depth at G6, the non-broken waves have steepened (with narrower, more pointed crests), and the the largest waves have broken.

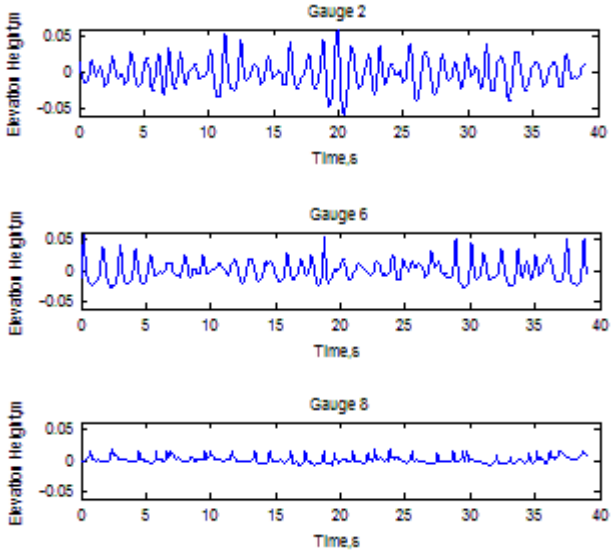

Figure 1. Surface elevation time histories in progressively shallow water depths at Gauges G2, G6 and G8 for Case A1a.

At the gauge in the shallowest depth, G8, almost all the waves have broken, and these progress up the beach as hydraulic bores. By this stage the maximum free surface elevation appears to have saturated at a limiting value.

Figure 2 presents the superimposed free surface elevation time histories containing the largest 10% crests. It can be seen that the profiles at G2 collapse onto a nearly constant wave shape for almost a typical wave period (i.e. ~ 1 s) either side of the maxima. At more distant times, the wave surface elevation behaviour loses its universality and appears to be almost random.

By G8, almost all the waves have broken, are effectively asymmetric, and have a fairly constant maximum elevation with time.

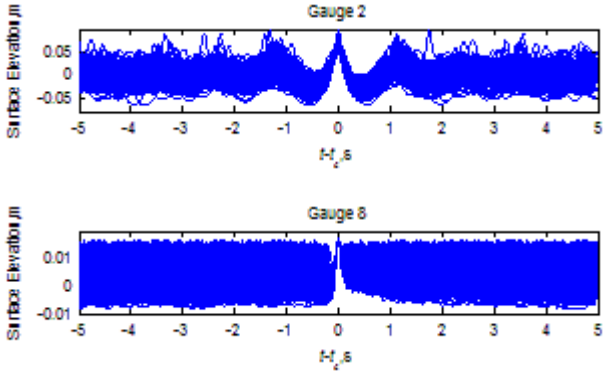

Figure 2. Case A1a: largest 10 % crest surface elevation time histories plotted relative to time the maximum surface elevation occurs (t - t_c). Upper plot: G2; lower plot: G8.

Figure 3 presents the averaged free surface with time for the 10% largest waves, with the time-reversed mirror image superimposed (in order to highlight symmetry). The largest crest events are quite symmetric at G2, but become increasingly asymmetric as the water shallows, due to the growth of wave nonlinearity until breaking occurs, after which the shape is saw-toothed.

Using Stokes theory, the free surface elevations averaged over the top 10 % of crest and troughs may be expressed as

$$\eta_c = S_0 A^2 + A\cos(\omega t) + S_2 A^2 \cos(2\omega t) + S_3 A^3 \cos(3\omega t) + \ldots + S_n A^n \cos(n\omega t) \quad (2)$$

and

$$\eta_t = S_0 A^2 - A\cos(\omega t) + S_2 A^2 \cos(2\omega t) - S_3 A^3 \cos(3\omega t) + \ldots + S_n A^n \cos(n\omega t) \quad (3)$$

in which η_c is the 10% largest crest averaged time series, η_t is the 10% largest trough averaged time series, S_i is a coefficient that defines the size of the i-th wave component, n is the number of components, A is the overall wave amplitude, ω is the wave angular frequency, and t is time. Of course, for an irregular wave train, the amplitude A and frequency ω are slowly varying functions of time, and the first term on the RHS of equations (2) and (3) is the slowly varying long wave

set-down term. Following Baldock et al. [8], Johannessen and Swan [10], Hunt et al. [14] and Borthwick et al. [15], the odd harmonics are given by

$$\frac{\eta_c - \eta_t}{2} = A\cos(\omega t) + S_3 A^3 \cos(3\omega t) + \ldots + S_{n-1} A^{n-1} \cos((n-1)\omega t) \quad (4)$$

and even harmonics by

$$\frac{\eta_c + \eta_t}{2} = S_0 A^2 \cos(0) + S_2 A^2 \cos(2\omega t) + \ldots + S_n A^n \cos(n\omega t) \quad (5)$$

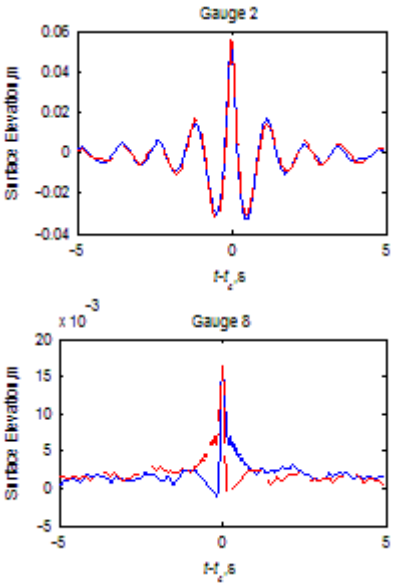

Figure 3. Case A1a: averaged 10 % largest-crest surface elevation time histories relative to time the maximum surface elevation occurs (t - t_c), and overlapped with reversed time.

By plotting the subtraction time series given by Equation (4) with the mirror image reversed time series (as shown in Figure 4), the odd harmonics exhibit symmetry in deep water (e.g. for Gauge G2) for depths reducing to 0.15 m, after which the methodology breaks down once the waves have broken.

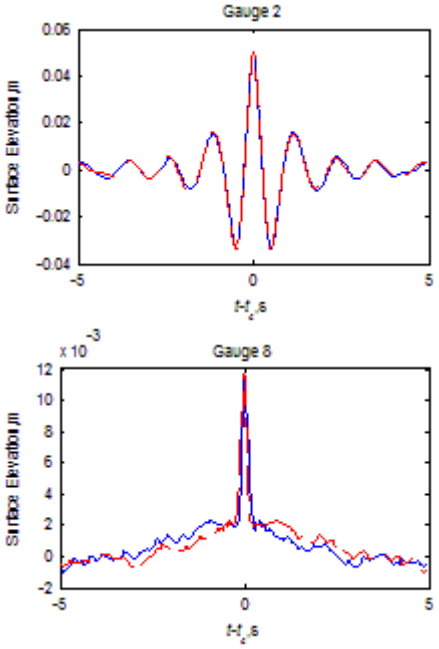

Figure 4. Case A1a: subtracted averaged 10 % crest-trough elevation [η_c - η_t]/2 time series relative to time maximum surface elevation occurs, overlapped with reversed time series.

Averaged crest- and trough-focused time series, which show the even wave harmonics are presented in Figure 5 for gauges G2 and G8. Before wave breaking occurs, the even harmonics contain a dominant component at half the first-order period (determined from the subtraction series). Post-breaking, the even harmonics are essentially anti-asymmetric.

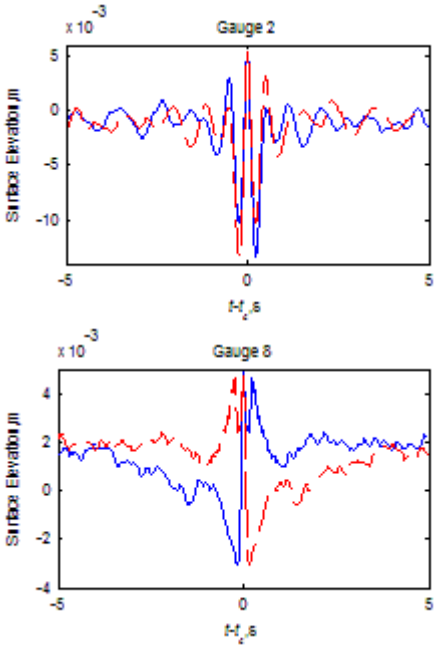

Figure 5. Case A1a: Added averaged 10 % crest-trough elevation [η_c + η_t]/2 time series relative to time maximum surface elevation occurs, overlapped with reversed time series.

Analysis of the extreme events in the free surface elevation time series obtained for the irregular waves in the Imperial College flume is useful in validating how well NewWave models the first-, second- and third-order wave components.

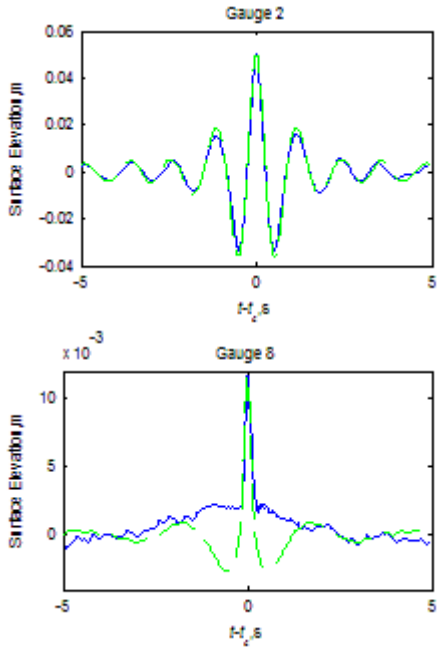

Figure 6. NewWave (with normalized height) compared with the average top 10 % average $[\eta_c - \eta_t]/2$ time series (blue line) for Case A1a, at G2 and G8.

Figure 6 illustrates the excellent fit obtained between NewWave (the height is normalized with the odd harmonics free surface elevation to compare the shapes) and the odd harmonic free surface elevation at G2, located offshore of the breaker line. There is a much poorer fit at G8, where all the primary waves have broken. For comparison in terms of magnitudes, the magnitudes of the linear and third-order harmonics are estimated from

$$\frac{\eta_c - \eta_t}{2} = A_1 \mathrm{NW} + A_3 \mathrm{NW}_3 \qquad (6)$$

in which

$$A_1 = \frac{\int \left(\frac{\eta_c - \eta_t}{2} \right) \mathrm{NW}\, \mathrm{d}t}{\int \mathrm{NW}^2\, \mathrm{d}t} \qquad (7a)$$

and

$$A_3 = \frac{\int \left(\frac{\eta_c - \eta_t}{2} \right) \mathrm{NW}_3\, \mathrm{d}t}{\int \mathrm{NW}_3{}^2\, \mathrm{d}t} \qquad (7b)$$

where

$$\mathrm{NW}_3 = \mathrm{NW}^3 - 3\mathrm{NW}_\mathrm{H}^2.\mathrm{NW} \ . \qquad (8)$$

In the foregoing, NW is the linear term, NW_3 is a representation of the third-order triple frequency term, and NW_H is the Hilbert transform of the NewWave time series. Figure 7 illustrates how well Equation (6) matches the $[\eta_c - \eta_t]/2$ time series [averaged with its time-reversed counterpart] for gauges up to up to G6 for Case A3e, being the most extreme case of all.

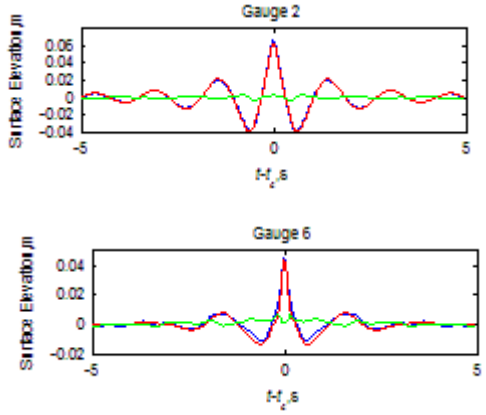

Figure 7. Time histories of averaged odd harmonics from the top 10 % crest- and trough focused wave groups (blue line), and linear (red line) and third (green line)-order NewWave terms for Case A3e, at G2 and G6.

A similar analysis is next performed for the even harmonics obtained from the addition of the crest- and trough-focused time series. This added series is first filtered to separate out the second-order sum and difference terms, and the magnitude of the filtered second-order term determined from

$$A_2 = \frac{\int \left(\frac{\eta_c - \eta_t}{2} \right) \mathrm{NW}_2\, \mathrm{d}t}{\int \mathrm{NW}_2{}^2\, \mathrm{d}t} \qquad (9)$$

in which

$$\mathrm{NW}_2 = \mathrm{NW}^2 - \mathrm{NW}_\mathrm{H}^2 \qquad (10)$$

where NW_2 is the second-order term. Figure 8 displays the close agreement obtained by the NewWave second-order component NW_2 to the filtered second-order sum components of the free surface time series at gauges G1 at d = 0.4 m and G7 at d = 0.1 m. Note that NW_2 has been normalised in terms of its height so that clear comparison can be made of the shape. From Equation (9), the percentage difference of magnitude between the two ranges from 5 % to 16 % for all gauges.

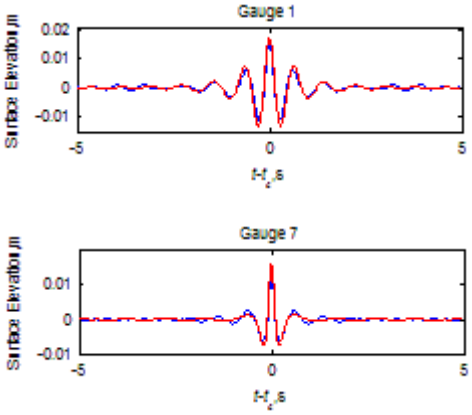

Figure 8. Time histories of averaged even harmonics from the top 10 % crest- and trough-focused wave groups (with normalized height), and Hilbert-transform approximation of NewWave terms (red line) for Case A3e at G1 and G7.

Returning to the Stokes expansion, by analogy with a regular wave train, we define modified Stokes coefficients, following Walker et al. [16] as) as $S_2 = S_{22}/d$ and $S_3 = S_{33}/d^2$, such that the free surface time series can be expressed in truncated form as

$$\eta = A\cos\theta + \frac{S_{22}}{d}A^2\cos 2\theta + \frac{S_{33}}{d^2}A^3\cos 3\theta . \quad (11)$$

From equations (6) and (11), it may deduced that

$$S_{22\mathrm{NW}} = \frac{A_2 d}{A^2} \quad \text{and} \quad S_{33\mathrm{NW}} = \frac{A_3 d^2}{A^3} . \quad (12)$$

A comparison between the experimental (Equation 12) and theoretical Stokes coefficients is shown in Figure 9, where it can be seen that the NewWave approximations and exact Stokes coefficients agree well over much of the range of kd values considered. There is no simple regular wave correction for the 2nd order difference component, but we do observe that each 2nd order double frquency term is associated with a difference term: each wave group propagates on a set-down (hole) of its own making.

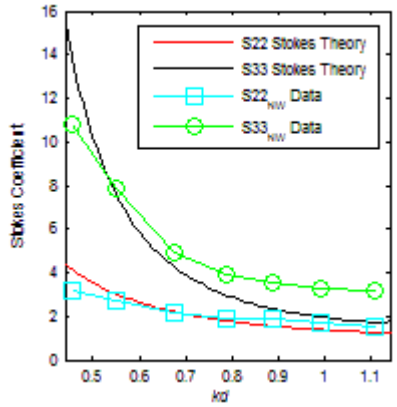

Figure 9. Stokes second- and third-order sum coefficients, S_{22} and S_{33}, plotted against kd.

3.2 *Breaking Waves*

For each case, the largest crest elevations, deepest troughs, and extreme wave heights were computed from the free surface time series. Figure 10 shows the non-dimensional maximum wave height ($H_{\max}k_\mathrm{p}$) and non-dimensional average height of the 10% largest waves ($H_{\max}k_\mathrm{p}$) as functions of the non-dimensional water depth ($k_\mathrm{p}d$). Here, k_p is the wave number corresponding to the deep water spectral peak period, T_p. The modified Miche limiting criterion given by Equation (2) is superimposed on Figure 10.

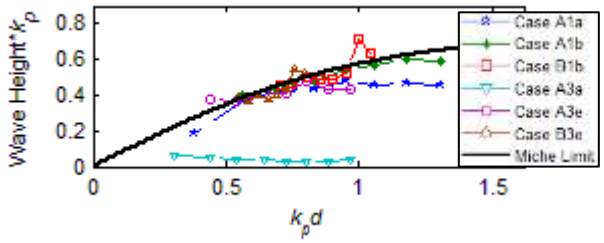

(a) Non-dimensional maximum wave height against non-dimensional depth

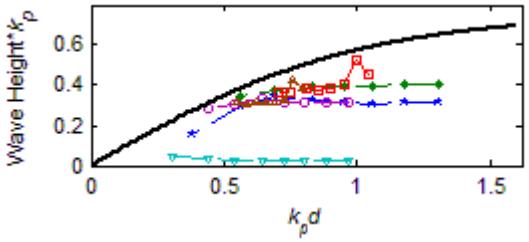

(b) Non-dimensional average value of 10% largest wave heights against non-dimensional water depth

Figure 10. Non-dimensional largest wave heights against non-dimensional water depth for Cases A1a, A1b, B1b, A3a, A3e and B3e, using the wave number, k_p, corresponding to the deep water spectral peak to non-dimensionalise the height and still water depth values.

It is obvious that the modified Miche criterion provides a limit to the maximum heights of broken waves.

3.3 *Broken Waves*

Once waves have broken, they cease to be dispersive, and behave more like solitary waves or hydraulic bores. This short section includes a simple analysis of both types of wave behaviour, and how well the analogies fit the measured data from the Imperial College laboratory flume.

The free surface motion of a solitary wave propagating over a steady, uniform current may be expressed using the Korteweg-de-Vries equation by

$$\eta = H + \mathrm{sech}^2\left[\frac{\sqrt{3}}{2}\left(\frac{H}{d^3}\right)^{1/2}(x - c't)\right] \quad (13)$$

where H is the height of the solitary wave, d is the still water depth, x is distance in the direction of propagation, c' is the modified solitary wave speed observed by a stationary observer, and t is time. In a current of speed u_c,

$$c' = c_{\mathrm{sol}} + u_{\mathrm{c}} \quad , \tag{14}$$

in which c_{sol} is the solitary wave speed in the absence of the current, given by

$$c_{\mathrm{sol}} = \sqrt{gd\left(1+\frac{H}{d}\right)}. \tag{15}$$

Figure 11 shows a fit of solitary wave theory (given by equations (13) to (15)) to the time history of the mean surface elevation of the top 20 crests at gauge G7 for kd = 0.56. The model appears reasonable for the single peak crest. This was not the case for kd < 0.4.

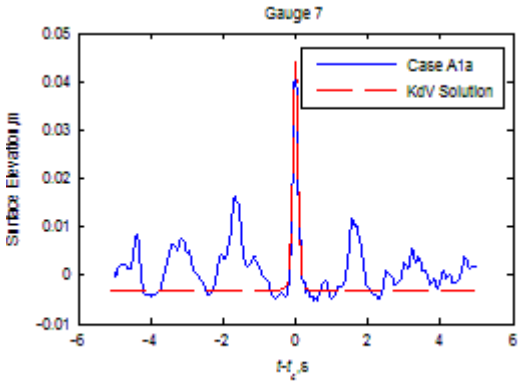

Figure 11. Solitary wave fitted to the mean of the surface elevation time histories corresponding to the top 20 crests for Case A1a at gauge G7. u_c is 0.6 ms^{-1}.

The alternative approach is to model the broken wave as a hydraulic bore. Following [17], a hydraulic bore travelling on a current of speed u_{c}, has a front speed given by

$$c' = c_{\mathrm{hj}} + u_{\mathrm{c}} \tag{16}$$

where c_{hj} is the speed the bore front would have in otherwise still water, and is given by

$$c_{\mathrm{hj}} = \sqrt{g(d+H)\left(1+\frac{H}{2d}\right)}. \tag{17}$$

Figure 12 presents a plot of the ratio of the modified front speed of broken waves modelled as bores to their corresponding front speeds in otherwise still water. The behaviour is reasonable, given that the front speed of a bore travelling on a current can be increased by up to 20%.

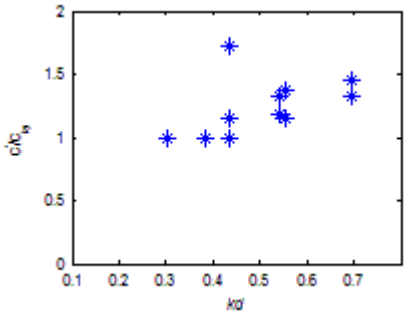

Figure 12. Non-dimensional effective wave speed for top 10 % of waves with each modelled as a hydraulic jump

4 CONCLUSIONS

This paper has presented an analysis of laboratory measurements of irregular waves propagating over mild bed slopes, characteristic of the continental shelf. Wave gauge data were interpreted in terms of the largest crest and trough events, and comparisons made with NewWave theory in deep water, a modified Miche criterion at breaking, and solitary wave theory and hydraulic bores for broken waves. From the raw data, it was observed that the wave crests sharpened and troughs widened during shoaling. In deep water, the wave time histories exhibited short term symmetry either side of a major event; this symmetry was lost once the waves broke.

NewWave was found to provide a reasonably accurate representation of the behaviour of the largest dispersive non-breaking waves in water of deep to intermediate depths, provided kd > 0.5. It was found that a truncated Stokes-like expansion gave a close approximation to the behaviour of extreme wave events in shoaling waters. By utilising a Hilbert-transformation approach, it was shown that NewWave gives an accurate representation of the magnitude and shape of second- and third-order components in irregular waves in the vicinity of maximum crests and troughs. These higher order contributions increased in magnitude as the depth reduced, until wave breaking occurred (for kd < 0.5), and NewWave theory no longer applied. Indeed, Katsardi et al. [13], have noted that the dispersive characteristics of the wave group is dominated by the effective water depth, kd. This factor becomes more important once the local significant wave height increases. The consequent increased nonlinearity of the wave group limits the applicability of the NewWave theory to larger effective water depths. For example, for the most nonlinear case examined in this paper (Case A3e, Table 1) NewWave theory can be applied with relative success up to kd > 0.75. The physical explanation for this lies in the effect of wave breaking and its dependence on both the wave steepness and the effective local water depth.

A modified Miche criterion was found to give an accurate upper bound estimate of maximum wave height, crest elevation and deepest trough elevation. At the point of breaking, the largest waves lost temporal symmetry as they changed abruptly into bore-like, non-dispersive waves. For the broken waves, either hydraulic bore or solitary wave theory should be appropriate, in which case the limiting wave height should be H_{max}/d = 0.754.

In short, designers of offshore structures located on the continental shelf should: (1) model non-broken extreme waves using NewWave, or similar, based on a specified offshore wave energy spectrum, provided $kd > 0.75$; (2) utilise the modified Miche criterion to estimate whether wave breaking has occurred; and (3) utilise the hydraulic bore analogy to model broken waves, though with caution as the fits to the data are less good than for the NewWave models for waves on deeper water.

ACKNOWLEDGMENTS

The LoWiSh Joint Industry Project (JIP) was sponsored by Shell International, Total, BP, ChevronTexaco, ConocoPhillips, ExxonMobil, Statoil, and Woodside Energy.

REFERENCES

[1] Lindgren, G. (1970), 'Some properties of a normal process near a local maximum', *The Annals of Mathematical Statistics*, 41, 1870-1883.
[2] Boccotti, P. (1983), 'Some new results on statistical properties of wind waves', *Applied Ocean Research*, 5(3), 134-140.
[3] Tromans, P.S., Anaturk, A., and Hagemeijer, P. (1991), 'A new model for the kinematics of large ocean waves – application as a design wave', *Proc. 1st Int. Offshore and Polar Engng Conf.*, Edin., U.K., 3, 64-71.
[4] Taylor, P.H., and Haagsma, I.J. (1994), 'Focussing of steep waves on deep water', *Proc. Int. Symp: Waves – Physical and Numerical Modelling*, Vancouver, Canada, Vol. 2, 862-870.
[5] Jonathan, P., and Taylor, P.H. (1997), 'Irregular, nonlinear waves in a spread sea', ASME, *J. Offshore Mech. Arct. Eng*., 119, 134–139.
[6] Taylor, P.H., Williams, B.A. (2004), 'Wave statistics for intermediate depth water - New waves and symmetry'. *Journal of Offshore Mechanics and Arctic Engineering*, 126 (1), 54-59.
[7] Rapp, R. J., and Melville, W. K., (1990), 'Laboratory measurements of deep water breaking waves', *Phil. Trans. R. Soc. A*, 331, 735–800.
[8] Baldock, T.E., Swan, C. and Taylor, P.H. (1996), 'A laboratory study of nonlinear surface waves on water', *Philos. Trans. R. Soc. Lond., A* 354: 649–676.
[9] Johannessen, T., and Swan, C. (2001), 'A laboratory study of the focusing of transient and directionally spread surface water waves', *Proc. R. Soc. London A*, 457, 971–1006.
[10] Johannessen, T. B., and Swan, C. (2003), 'On the nonlinear dynamics of wave groups produced by the focusing of surface-water waves', *Proc. R. Soc. A*, 459, 1021–1052.
[11] Miche, R. (1944), ' Undulatory movements of the sea in constant and decreasing depth', *Ann. De Ponts et Chaussees* (May-June, July-August): 25-78, 131-164, 270-292, 369-406.
[12] Katsardi, V. (2009) *Surface water waves in intermediate and shallow water depths*. PhD dissertation, Imperial College, London.
[13] Katsardi, V, de Lutio, L., and Swan C. (2013), 'An experimental study of large waves in intermediate and shallow water depths. Part I: Wave height and crest height statistics', *Coastal Engineering*, 73: 43-57.
[14] Hunt, A.C., Taylor, P.H., Borthwick, A.G.L. and Stansby, P.K. (2005), 'Phase inversion and the identification of harmonic structure in coastal engineering experiments', *Proceedings of ASCE 29th International Conference on Coastal Engineering*, Lisbon, 1047–1059.
[15] Borthwick, A.G.L., Hunt, A.C., Feng, T., Taylor, P.H. and Stansby, P.K. (2006), 'Flow kinematics of focused wave groups on a plane beach in the U.K. Coastal Research Facility', *Coastal Engineering*, 53(12), 1033-1044.
[16] Walker, D.A.G., Taylor, P.H., and Eatock Taylor R. (2004), 'The shape of large surface waves on the open sea and the Draupner New Year wave', *Applied Ocean Research*, 26, 73-83
[17] Chow, V.T. (1985) *Open-channel Hydraulics*, 21st Printing, McGraw-Hill, Singapore, 1985.